Case Studies in Thermal Engineering 35 (2022) 102137

Contents lists available at ScienceDirect

Case Studies in Thermal Engineering

journal homepage: www.elsevier.com/locate/csite

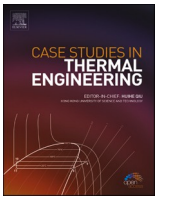

Energy performance enhancement in air-source heat pump with a direct evaporative cooler-applied condenser

Beom-Jun Kim, Su-Young Jo, Jae-Weon Jeong *

Department of Architectural Engineering, College of Engineering, Hanyang University, Seoul, 04763, Republic of Korea

A R T I C L E I N F O

Keywords:
Air-source heat pump
Direct evaporative cooler
Optimal system operation
Outdoor air condition
Energy-saving potential

A B S T R A C T

The energy consumption of the air-source heat pump operated in cooling mode is affected by the outdoor air condition in summer. It is important to not only install the evaporative cooler in front of the condenser inlet side but also consider the operation strategy of the evaporative cooler under the hot and humid condition. In this study, the energy saving potential of the air-source heat pump with an evaporative cooler was analyzed according to the operation strategy. A three-story office building measuring 100 m^2, using an enthalpy recovery ventilator, was used as a model building conditioned by the proposed system for detailed energy simulation. The building thermal load and energy consumption were estimated using simulation tools. The results show that the proposed system reduces 8.87% of energy consumption compared with the conventional air-source heat pump when the evaporative cooler operated under the 72% of relative humidity condition.

Nomenclature

A_z	Zone area [m^2]
CMH	Cubic meter per hour [m^3/h]
c_p	Specific heat [kJ/kg ° C]
E_z	Zone air distribution effectiveness [−]
g	Gravitational acceleration [m/s^2]
Head	Head loss [m]
h	Enthalpy [kJ/kg]
$\dot{m}$	Mass flow rate [kg/s]
P	Power [kW]
P_z	People [−]
$\dot{Q}$	Heat rate [kW]
R_p	Outdoor area air rate [−]
T	Temperature [° C]
$\dot{V}$	Velocity [m/s]
$\dot{W}$	Power [kW]

* Corresponding author.
E-mail address: jjwarc@hanyang.ac.kr (J.-W. Jeong).

https://doi.org/10.1016/j.csite.2022.102137
Received 24 February 2022; Received in revised form 11 May 2022; Accepted 21 May 2022
Available online 25 May 2022

Greek Symbols

α	Relative humidity effectiveness of desiccant wheel [−]
ε	Efficiency [−]
η	Effectiveness [−]
ρ	Density [kg/m^3]
ω	Humidity ratio [kg/kg]

Subscripts

a	Air
amb	Ambient
comp	Compressor
cond	Condenser
dbt	Dry-bulb temperature
dec	Direct evaporative cooler
EX	Enthalpy exchanger
evap	Evaporator
hx	Heat exchanger
i	Inlet
lat	Latent heat
o	Outlet
oa	Outdoor air
p	Static pressure
ref	Refrigerant
sa	Supply air
sen	Sensible heat
sp	Superheat
tot	Total
vent	Ventilation
wb	Wet-bulb

Abbreviations

CHP	Combined heat and power
COP	Coefficient of performance
DBT	Dry-bulb temperature
ERV	Enthalpy recovery ventilator
HVAC	Heating, ventilation & air-conditioning

1. Introduction

HVAC systems use heat pump systems to save energy. The heat pump can transfer heat from a low-temperature heat source to a high heat-temperature source using the latent heat of the refrigerant [1]. A building can be cooled by releasing the heat from inside to the outside [2] using a heat pump. The research on HVAC systems using a heat pump has been an important topic for the building sector, and many studies have been conducted earlier [3–5].

The heat absorbed from a room being cooled is released outside the building by heat exchange owing to the temperature difference between indoor air and outdoor air. However, due to the high outside temperature in summer, the heat release performance of the condenser deteriorates. A recent report on global climate change by the IPCC states that the global surface temperature will continue to rise in the coming decades [6]. To maintain the heat release performance at high ambient temperatures, the temperature set for the outdoor condenser should be increased. A higher refrigerant compression is required to increase the heat-dissipation temperature. More energy is required to increase the compressibility of the refrigerant, leading to the higher energy consumption of the building.

This problem can be mitigated by installing a direct evaporative cooler in front of the condenser. Evaporative cooling is when water evaporates from a liquid state to a gaseous state while absorbing the heat of evaporation, removing the surrounding heat [7,8]. When water is sprayed into the air, the temperature of the air is cooled owing to the evaporation of water. When the cooled air flows into the condenser, the temperature difference between the condenser and the air increases, and thus the heat dissipation performance is improved. Previous studies using numerical and experimental analyses of evaporative cooling-based air-source heat pumps have been conducted [9–14]. Experimental verification of evaporative cooling-based heat pump system has been conducted. Youbi-Idrissi et al. [9] developed a semi-local mathematical model of an air-cooled condenser, with and without spraying water, to evaluate the system performance. The result showed that the cooling capacity and COP of the water sprayed condenser increased by 13% and 55%, respectively, than the dry air-cooled condenser. Hajidavalloo and Eghtedari [10] studied an evaporative cooler coupled to an existing air-cooled condenser and measured the effect on the heat pump cycle performance under hot ambient air conditions. Experimental

results showed that the power consumption can be reduced by 20%, and COP improved by 50%. Jahangeer et al. [11] numerically analyzed an evaporative cooled condenser using the finite-difference technique. Several experimental studies have been conducted to validate the performance of evaporative cooling condensers [12,13]. Sarnichartsak and Thepa [12] predicted the performance of an air conditioner with an evaporative cooled condenser, and their models satisfied the test data. Wang et al. [13] conducted an experimental investigation of an air-conditioning system using an evaporative cooling condenser. The system COP increased from 6.1% to 18%, and the compressor's power consumption reduced by 14.3%. Martinez et al. [14] studied the impact of different cooling pads on the overall performance of an air-conditioning system with an evaporative cooler. The experiments were conducted with variable-thickness cooling pads, and the improvements in power consumption and overall COP were evaluated. Recently, a few studies were investigated to enhance the evaporative condenser by experimental and numerical analysis. Pan et al. [15] introduced a novel water-cooling centralized air conditioning system in the subway. They installed two types of air ducts, and the result indicates that the evaporative condenser-air conditioner can enhance energy efficiency and reduce operation costs and carbon emissions. Yang et al. [16,17] experimented spray type of evaporative condenser. They investigated the impact of arrangement of spraying mode and nozzle position [16] and the influence of different outdoor temperatures, mass flow rates of nozzles and operation modes of the proposed system [17]. Ketwong et al. [18] analized the evaporative cooled condenser in different hot-dry and hot-humid climates. The result showed that energy efficiency ratios for hot–dry and hot–humid climates ranged from 3.40 to 4.22 and 3.30 to 3.94, respectively, compared to 3.01 for the normal unit. Li et al. [19] proposed a novel household ventilator with indirect evaporative cooling system to enhance the exhaust air heat pump. The proposed system was tested with four different operation modes.

Previous studies have focused on the mechanical performance evaluation of a heat pump system installed with a direct evaporative cooler on the laboratory scale. However, when an evaporative cooling condenser with a heat pump system is used in an office building, unlike the lab-scale experiment, the performance improvement of the system must be evaluated considering the various outside air conditions. In particular, the evaporative cooler is affected by the humidity of the air at the inlet side of the condenser. Therefore, if the system is used to cool the building, the energy performance evaluation of the proposed system should be conducted considering the office occupancy schedule, zone load, and outdoor air conditions. However, limited studies have been conducted on building applications. Shen et al. [20] studied the energy and economic analyses of an evaporative cooled condenser for building and refrigerant systems in various climates. This study simulated the proposed system applied to a building in 16 different climate zones for three types of buildings, and the results were compared for each climate and building type. The proposed system operates depending on the one-point air condition.

Therefore, this study investigated the optimal operation strategy of an air-source heat pump system with a direct evaporative cooler installed in an office building. The HVAC system of the building was assumed to consist of an indoor air conditioning system (e.g., an air-source heat pump) and a ventilation system (e.g., enthalpy exchange ventilator). The energy simulation was conducted by applying the occupancy schedule, ventilation rate, and annual ambient air condition data. The operation analysis was conducted during summer to focus on the systems cooling performance.

2. System description

2.1. Direct evaporative cooler assisted condenser

An air-source heat pump system is the most used air conditioning system in office buildings [21]. It comprises an evaporator, condenser, compressor, expansion valve, and four-way valve [1]. In summer, the heat pump operates in the cooling mode to reduce the cooling load in the target zone of the office building. The cooling and dehumidification processes for indoor air in an office is conducted using a heat pump, located in the indoor section, in which, heat exchange takes place between the refrigerant and the air in the evaporator. In this situation, the hot and compressed refrigerant absorbs heat from the ambient air. Evaporation causes the air in the zone to cool and dehumidify when the air is cooled below the dew point. Here, the refrigerant inside the evaporator flows in a low-temperature and low-pressure state as it passes through the expansion valve, promoting the heat exchange with the indoor air. The vaporized refrigerant passes through the compressor to a high-temperature and high-pressure state. Continuous indoor cooling requires the gaseous refrigerant to be converted back to the liquid state. To condense the refrigerant, the high-temperature and high-pressure refrigerant flows into the condenser located outside. The condenser introduced the outdoor air and released condensation heat through heat exchange with the refrigerant. Once all the condensation heat is released, the refrigerant liquifies and flows back into the expansion valve to continue the cooling cycle.

Because the air-source heat pump uses outdoor air as a heat sink, the outdoor temperature and humidity conditions significantly affect the performance of the heat pump. Therefore, a certain temperature difference between the condensing temperature of the refrigerant and the outside air should be maintained. If the outside temperature increases, the condensing temperature of the refrigerant increases. An increase in the condensing temperature of the refrigerant increases the compression rate. Thus, power consumption increases as the compressor ratio increases. Therefore, in summer, the compressor consumes higher energy. These phenomena can lead to significant energy use in the summer.

Direct evaporative cooling is a simple method for solving this performance degradation phenomenon of the heat pump system. When the water vaporizes, it cools the introduced air as the water removes heat from the ambient air. The ambient air can be cooled until the wet-bulb temperature is reached. The wet-bulb temperature is the point at which water can evaporate to the maximum level. The air temperature of the cooled air can be calculated using the efficiency equation (Equation (1)). Based on a previous experimental study [22], the heat exchange efficiency of the direct evaporative cooler was set to 0.8.

$$T_{a.dec} = T_{a.amb} - \varepsilon_{dec}(T_{a.amb} - T_{wb.a.amb}) \quad (1)$$

Outdoor air enters the condenser drawn through the condenser fan. Heat exchange between the refrigerant and air takes place in the condenser ($\dot{m}_{a.coond}$). In a conventional condenser without an evaporative cooler, the amount of heat dissipation can be calculated as follows:

$$\dot{Q}_{outdoor} = \varepsilon_{hx}\dot{m}_{a.cond}c_p(T_{cond} - T_{a.outdoor}) \tag{2}$$

The heat dissipation ($\dot{Q}_{outdoor}$) of the condenser was determined by multiplying the specific heat of the air (c_p) by the mass flow rate of the introduced air ($\dot{m}_{a.coond}$), the temperature difference between the condensing temperature (T_{cond}) and the condenser ambient air ($T_{a.outdoor}$). The actual amount of heat dissipation of the condenser was determined by the efficiency (ε_{hx}) of the condenser coil. As the temperature of the air decreased, the released heat increased. Assuming that the heat dissipation is constant, the energy consumption can be reduced by decreasing the temperature of the condenser. The compressor can lower the compressor ratio, reducing the temperature. Conversely, if the ambient air in the building is cooled by the evaporative cooler and flows into the condenser ($T_{a.dec}$), heat dissipation can be maintained even if the condensing temperature is maintained or reduced ($T_{cond.new}$). The treated air temperature ($T_{air.dec}$) cooled by the evaporation of water is determined by the efficiency of the evaporative cooler, assuming that it can ideally be cooled to the wet-bulb temperature of the ambient air. Therefore, it is possible to operate the condenser by reducing the temperature (Equations (3) and (4)). This leads to a reduction in the compression ratio of the compressor, thereby reducing the energy consumption. These equations are expressed as follows.

$$\dot{Q}_{outdoor} = \varepsilon_{hx}\dot{m}_{a.cond}c_p(T_{cond.new} - T_{a.dec}) \tag{3}$$

$$T_{cond.new} = T_{a.dec} + \frac{\dot{Q}_{outdoor}}{\varepsilon_{hx}\dot{m}_{a.cond}c_p} \tag{4}$$

2.2. Proposed system overview

Fig. 1 shows an HVAC system consisting of ventilation and a heat pump air-conditioning system. The ERV system handles ventilation in the zone. The enthalpy exchanger is used to reduce the ventilation load by exchanging the enthalpy with the outdoor air and exhaust air from the zone [23]. The ERV uses its heat exchange efficiency to calculate the temperature and humidity ratio of the processed air after heat exchange (Equations. 5 and 6). The cooled and dehumidified air was discharged using the ceiling duct. The processed ventilation air was supplied through a diffuser installed on the zone's ceiling. The supply air heat can be calculated using the following equation (Equation (7)):

$$T_{sa.EX} = T_{oa} - \varepsilon_{EX.sen}(T_{oa} - T_{zone}) \tag{5}$$

$$\omega_{sa.EX} = \omega_{oa} - \varepsilon_{EX.lat}(\omega_{oa} - \omega_{zone}) \tag{6}$$

$$\dot{Q}_{sa} = \dot{m}_{vent}c_{pa}(T_{zone} - T_{sa}) \tag{7}$$

The zone thermal load remaining can be determined by subtracting the total zone thermal load from the heat of the supply air. Therefore, the cooling load of the indoor evaporator can be calculated using the following equation (Equation (8)).

$$\dot{Q}_{zone} = (\dot{Q}_{total} - \dot{Q}_{sa}) \tag{8}$$

If thermal load in the zone persists after supplying ventilation air, the air-source heat pump is operated. The evaporator of the heat pump located indoors cooled the zone air to remove the total heat load. A condenser located on the outdoors side is used to release heat absorbed by the evaporator. A direct evaporative cooler was installed in front of the condenser. Both the air-source heat pump and the

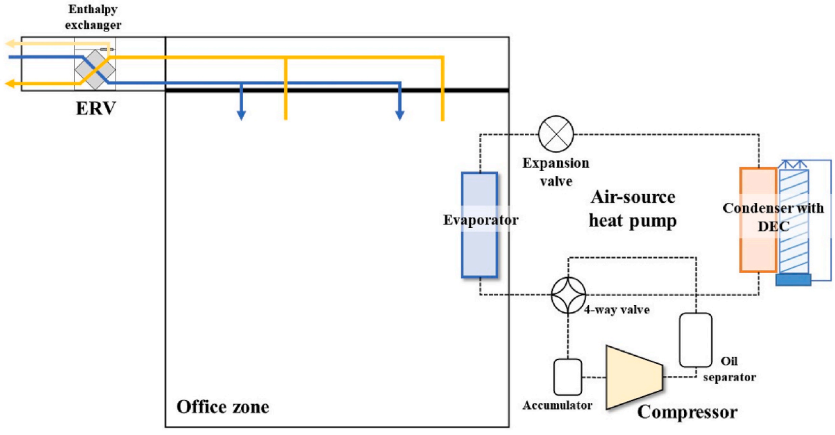

Fig. 1. Schematic diagram of air-source heat pump cooling system for building zone.

direct evaporative cooler were activated together. The air supplied to the condenser cools the outdoor air closer to the wet-bulb temperature to improve the heat release performance of the condenser.

2.3. System operation

The objective of this study is to investigate the energy consumption is affected by the summer operation of the HVAC system (e.g., ERV and air-source heat pump) installed in an office building with a direct evaporative cooler installed in front of the condenser. Therefore, it is important to understand the operation mode and working flow of each component considering the condition of the air, both indoors and outdoors, and the heat load of the building.

(1) ERV

The operation mode of the ERV is determined based on the conditions of indoor air and air supply. The indoor air conditions refer to the enthalpy line and dry-bulb temperature (DBT) line based on 26 °C and 50% relative humidity as indoor conditions during summer [24]. The DBT was set to 15 °C. When cooling the zone based on these lines, the outdoor air conditions can be divided into three modes on the psychrometric chart. In Mode A, it is advantageous to reduce the ventilation load bypassing the enthalpy exchanger when the outdoor air condition is greater than the indoor enthalpy and DBT line. This is because the enthalpy is exchanged between the outdoor and indoor air in the enthalpy exchanger. In Mode B, the indoor air is exhausted, without heat exchange, through the bypass duct of the enthalpy exchanger. Because the outdoor air condition is lower than the indoor condition lines, it is disadvantageous to exchange heat with the indoor air. In Mode C, if the outside air is colder than the supply condition set for cooling and is supplied to the room untreated, it may cause discomfort and a cold draft to the occupants. Therefore, the air is heated using the enthalpy exchanger.

(2) Heat pump

Fig. 2 shows the operation logic, during summer, of the air-source heat pump. The heat pump operation logic, proposed in this study, is controlled by the indoor air supply condition, outdoor in-out temperature difference, and air volume conditions. For heat pump control, it is assumed that the indoor and outdoor units have a temperature difference of up to 10 °C for heat exchange. In addition, it is assumed that the basic indoor and outdoor air volumes do not exceed 1000 CMH.

First, the designed outlet temperature of the indoor evaporator was determined assuming ($T_{sa.design}$). To remove the remaining indoor thermal load after ventilation, the air volume of the heat pump indoor unit (m_{sa}) (Equation (9)) was calculated. It is converted into CMH to determine the appropriate supply air conditions (Equation (10)). If the air volume exceeds 1000 CMH, the air volume is assumed to be 1000 CMH. This prevents excessive indoor air volume operations. If it exceeds 1000 CMH, the supply air temperature is calculated using the corresponding mass flow rate (Equation (11)). Otherwise, the calculated mass flow rate is determined as the indoor supply air mass flow rate; the supply air temperature is calculated at this point (Equation (11)). If the actual calculated supply air temperature is lower than 5 °C, the supply air temperature is fixed at 5 °C, and the supply air mass flow is recalculated. The

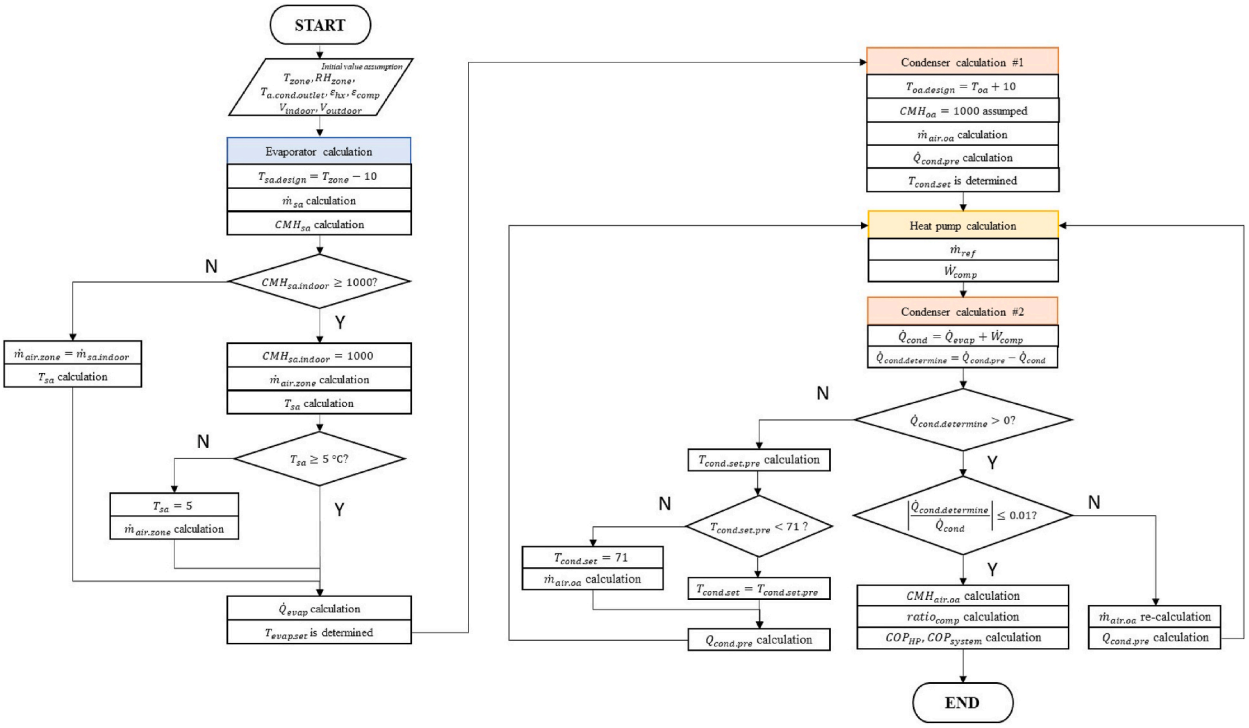

Fig. 2. Flow chart of the calculation logic of the heat pump system in the proposed system.

temperature is fixed to prevent a cold draft to the occupants. In this state, the supply air mass flow rate, supply air set temperature, supply air specific heat, and indoor set temperatures are determined. The remaining indoor heat load after ventilation air was supplied was chosen as the evaporator load (Q_{evap}). The evaporation temperature of the heat pump refrigerant must be determined ($T_{evap.\ set}$) (Equations (12) and (13)). The equations for the evaporation temperature are as follows:

$$\dot{m}_{sa} = \frac{\dot{Q}_{zone}}{c_{p.sa}\left(T_{zone} - T_{sa.design}\right)} \tag{9}$$

$$CMH_{sa} = \frac{\dot{m}}{\rho_{sa}} \times 3600 \tag{10}$$

$$T_{sa} = T_{zone} - \frac{\dot{Q}_{zone}}{\dot{m}_{sa} c_{p.sa}} \tag{11}$$

$$\dot{Q}_{evap} = \dot{m}_{sa} c_{p.sa} \left(T_{zone} - T_{sa}\right) \tag{12}$$

$$T_{evap.set} = T_{zone} - \frac{\dot{Q}_{evap}}{\varepsilon_{hx} \dot{m}_{air.zone} c_{p.sa}} \tag{13}$$

The outdoor condensation temperature of the heat pump determines the design condition above an inlet temperature of 10 °C based on the assumptions ($T_{oa.design}$). It was assumed that the air volume of the outdoor unit was fixed and operated at 1000 CMH. After calculating the mass flow rate ($m_{air.oa}$) (Equation (14)), the amount of heat release rate required for heat dissipation ($Q_{cond.pre}$) (Equation (15)), and the condenser temperature of the heat pump ($T_{cond.set}$) (Equation (16)).

$$\dot{m}_{air.oa} = \frac{CMH_{oa} \rho_{oa}}{3600} \tag{14}$$

$$\dot{Q}_{cond.pre} = \dot{m}_{air.oa} c_{p.oa} \left(T_{oa.design} - T_{oa}\right) \tag{15}$$

$$T_{cond.set} = T_{oa} + \frac{\dot{Q}_{cond.set}}{\varepsilon_{hx} \dot{m}_{air.oa} c_{p.oa}} \tag{16}$$

After both the indoor evaporator refrigerant and outdoor condenser refrigerant temperatures are determined, thermodynamic equations are evaluated. First, the amount of refrigerant required for indoor cooling (m_{ref}) is determined (Equation (17)). Then, the compressor work is determined based on the thermodynamic equation (W_{comp}) (Equation (18)). The compression ratio of the compressor was assumed to be 0.75 [25]. After calculating the heat of the condenser (Q_{cond}) to maintain the heat balance (Equation (19)), it is compared with the required heat release rate ($Q_{cond.determine}$) (Equation (20)). First, we calculate the difference between the heat release rate of the outdoor unit and that calculated by the heat balance equation. Next, we verify whether the difference (i.e., error range) is within 1%. If the error range is positive (i.e., heat release rate greater than value from heat balance equation) then we calculate the entire system's energy, outdoor unit fan CMH, compression ratio, and COP of the heat pump. If the calculated outdoor unit heat release exceeds the 1% error range from the heat balance equation, the outdoor unit air volume is altered to recalculate the heat release rate using the air volume control. Subsequently, the error value is reduced by restarting the heat pump calculation process based on the change in the volume of heat dissipated by the outdoor unit. If the value computed using the heat balance equation is greater than the observed value, and if the observed heat release rate is negative, the condenser temperature setting is changed to increase the actual heat release ($T_{cond.set.pre}$). The R410a refrigerant was used in this study, and the refrigerant temperature at the critical point was 71 °C. The condenser refrigerant temperature setting was noted when the refrigerant temperature was less than 71 °C. Thereafter, the condensers heat release is recalculated, and the error is reduced by comparing the actual calculated heat release rate and the heat calculated by the heat balance equation.

$$\dot{m}_{ref} = \frac{\dot{Q}_{evap}}{h_{evap.o.sp} - h_{evap.i}} \tag{17}$$

$$\dot{W}_{comp} = \dot{m}_{ref} \left(h_{comp.o.act} - h_{comp.i}\right) \tag{18}$$

$$\dot{Q}_{cond} = \dot{Q}_{evap} + \dot{W}_{comp} \tag{19}$$

$$\dot{Q}_{cond.determine} = \dot{Q}_{evap.pre} - \dot{Q}_{cond} \tag{20}$$

(3) Direct evaporative cooler

The basic method for calculating the temperature of the air passing through the evaporative cooler is to calculate based on ratio of the actual cooling per ideal cooling determined with wet-bulb temperature. The lowest temperature to which the air can be cooled by

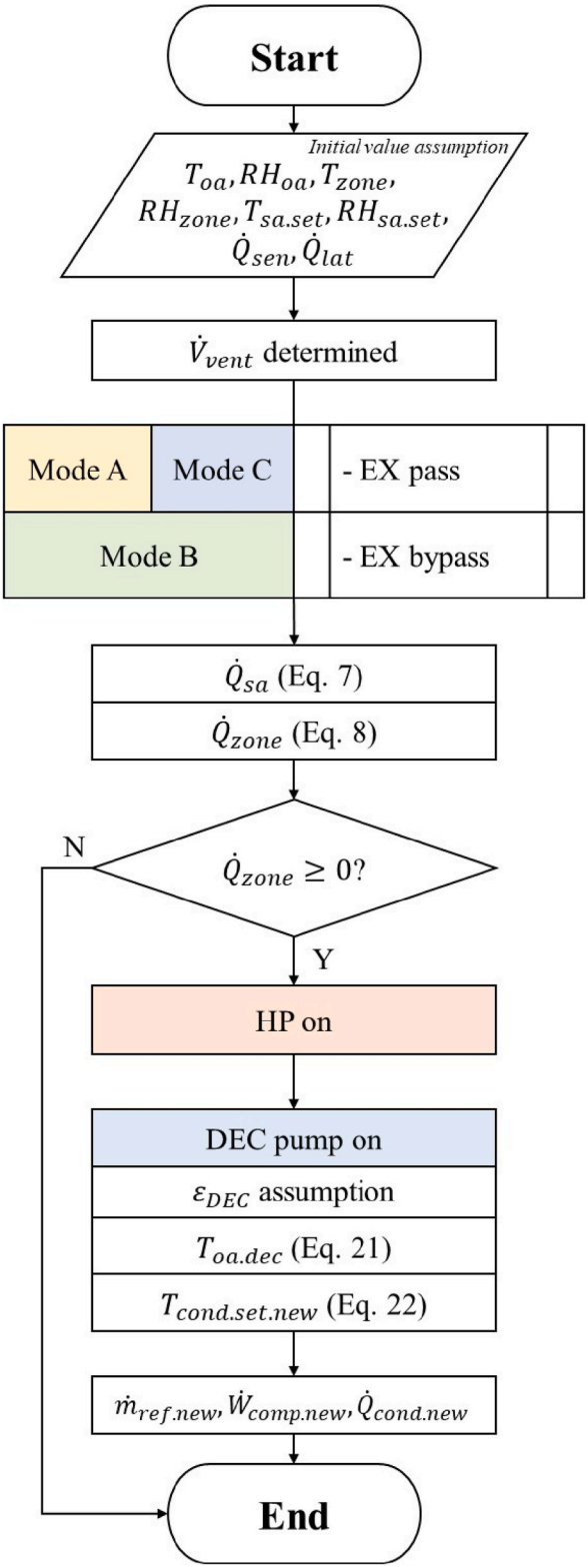

Fig. 3. Flow chart of the proposed system operation.

evaporative cooling depends on the efficiency of the evaporative cooler. Assuming that the evaporative cooling efficiency is 0.8 [26], the outlet air temperature passing through the evaporative cooler is calculated using Equation (21). Because the cooling air temperature is the same as the inlet air temperature of the outdoor unit of the heat pump, the set condenser refrigerant temperature can be determined by the modified condenser inlet air temperature (Equation (22)). The heat pump and the direct evaporative cooler unit are operated together. When the direct evaporative cooler was operated

$$T_{oa.dec} = T_{oa.dbt} - \varepsilon_{dec}(T_{oa.dbt} - T_{oa.wbt}) \tag{21}$$

$$T_{cond.set.new} = T_{oa.dec} + \frac{\dot{Q}_{cond}}{(\varepsilon_{dec}\dot{m}_{air.oa}c_{p.oa})} \tag{22}$$

(4) Flow chart assembly

Fig. 3 shows the operation logic flow for handling all the components. First, the ERV calculated the amount of indoor ventilation. The corresponding indoor ventilation was the minimum ventilation standard according to ASHRAE Standard 62.1 [27]. Subsequently, the mode is selected according to the external air condition. After calculating the ERV according to the proposed mode, the amount of heat supplied was calculated, and the amount of heat remaining in the room was calculated. If the amount of heat remaining in the room was less than zero, the system operation was terminated because the entire heat load in the room was captured by ventilation. If the remaining heat load in the room was greater than zero, the heat pump calculation was repeated according to the heat pump calculation logic (Fig. 3). After calculating the air condition (cooled by evaporative cooling by operating the direct evaporative cooler), the set condenser refrigerant temperature of the heat pump was corrected to recalculate the corrected refrigerant amount, compressor energy consumption, and condenser heat dissipation.

3. Simulation overview

3.1. Model building

A three-story office building in Seoul was simulated in this study. A floor area of 100 m^2 was used in the simulation. The settings of the simulated model building are listed in Table 1 [28]. The performance of the building was based on the energy conservation standards published by the government [29]. The temperature and humidity conditions in the zone were assumed to be 26 °C and 50%, respectively. The humidity ratio of air was calculated to maintain this condition. Based on the above conditions, the practical and latent heat loads of the model building were calculated using the TRNSYS program [30].

3.2. System assumption

The purpose of this paper was to evaluate the energy performance of the proposed system with different operation strategy during summer. To analyze the system energy simulation, we made several assumptions as follows:

1) Hourly simulations
2) Adiabatic cooling system
3) Steady-state simulation was assumed in this paper

3.2.1. Air-source heat pump

Characteristics of the designed air conditions and heat pump system are listed in Table 2. Design parameters were selected based on the hottest hours in summer. The airflow rate of each component was calculated based on the designed air conditions. The refrigerant

Table 1
Simulation input values of model building [28].

Regime types	Parameters	Values
Floor area		100 m^2
Number of floors		3
Occupants		15
Simulation period		June–September (Cooling season)
Location		Seoul
Zone condition	Temperature	26 °C
	Relative humidity	50%
Supply air condition	Temperature	15 °C
	Relative humidity	80%
Heat gain	People	130 W/person (sensible, latent)
	Equipment	7 W/m^2
	Lights	12.5 W/m^2
U-value	Outdoor wall	0.240 W/m^2K
	Floor	0.276 W/m^2K
	Roof	0.141 W/m^2K
	Window	1.4 W/m^2K

Table 2
Air condition and heat pump system characteristics in the design condition of the simulation.

Parameters	Min	Average	Max
Outdoor air temperature [°C]	13.4	23.6	33.5
Outdoor air relative humidity [%]	36.5	76.0	100.0
Indoor air temperature [°C]	26.0	26.0	26.0
Indoor air relative humidity [%]	50.0	50.0	50.0
$\dot{V}_{vent}$ **[CMH]**	110.2	127.2	150.8
$\dot{V}_{oa}$ **[CMH]**	33.7	851.5	1707.0
$\dot{V}_{indoor}$ **[CMH]**	31.7	816.8	1474.0
Refrigerant ton	0.4	13.1	38.2
Horsepower	0.0	1.0	6.6
Coefficient of performance	1.0	5.4	9.3

tonnage and horsepower of the heat pump were determined using the designed conditions. The seasonal energy efficiency ratio was calculated from the sum of the cooling capacity and input electrical power.

3.2.2. Direct evaporative cooler

Manufacturer's catalog [31] information was used to set the water pump parameters, namely, water was sprayed at 60 L/min on the upper surface of the pad. The water temperature was fixed at 25 °C. The effectiveness of the evaporative cooling pad was set to 0.8 based on an experimental study [32,33]. It was assumed that the heat exchanger was insulated.

3.3. Ventilation rate

Ventilation air was introduced according to the minimum ventilation rate based on the ASHRAE Standard 62.1 [27]. The equation of the ventilation mass flow rate consists of the outdoor air rate (R_p) multiplied by the person (P_z), area outdoor air rate (R_a) multiplied by the zone area (A_z), and zone air distribution effectiveness (E_z). An office as assumed as the target zone.

$$\dot{m}_{vent} = \left(R_p \times P_z + R_a \times A_z\right)/E_z \tag{23}$$

3.4. Fan and pump

The system proposed in this study requires four fans, located at the supply and return sides of the ERV, indoor air conditioner, and the outdoor unit. The airflow rate of each fan ($\dot{V}_{design}$) was calculated using the ERV, indoor unit, and outdoor unit air mass flow rate equations [34]. A fan efficiency of 50% was used in this study. The pressure drop was derived based on previous studies [35,36]. The pressure drop value and the thickness, assumed in this study, were based on the manufacturer's catalog [31]. The pressure drop values of the system components are listed in Table 3. Fan energy consumption was determined based on the following equations (Equations (24)–(26)) [37]:

$$P_{fan.design} = \frac{\dot{V}_{design} \sum \Delta P}{\eta_{fan}} \tag{24}$$

$$P_{fan} = \left(0.0013 + 0.1470 PLR_f + 0.9506 PLR_f^2 + 0.0998 PLR_f^3\right) \times P_{fan.design} \tag{25}$$

$$PLR_f = \frac{\dot{V}_{current}}{\dot{V}_{design}} \tag{26}$$

A *direct evaporative cooler* (Section 3.2.2) was used in this study. Water was sprayed at 60 L/min on the upper surface area of the pad as described in the manufacturer's catalog ($\dot{V}_{water}$). The design pump head loss (*Head*) was assumed to be 15 m, and the pump efficiency (η_{pump}) was 60%. The energy consumption of the pump was calculated as follows:

$$P_{pump} = \frac{\dot{V}_{water} \times g \times Head}{\eta_{pump}} \tag{27}$$

Table 3
Pressure drop of system components.

Components	Pressure drop (Δp)
Heat exchanger	250 Pa
Enthalpy exchanger	100 Pa
Direct evaporative cooling pad	20 Pa
SA duct balance	500 Pa
EA duct balance	500 Pa

4. Simulation result and discussion

4.1. System performance

4.1.1. Outdoor air condition

The outdoor air condition was plotted on a psychrometric chart to assess the conditions of the outdoor air passing through the direct evaporative cooler (Fig. 4). Compared with the conditions of the outdoor air during the summer, which are widely distributed, the air condition converges to a certain condition after passing the evaporative cooler. An evaporative cooler, used during the summer, can maintain air conditions in which temperature does not exceed 27.7 °C.

The air condition data, in Seoul, for the summer of 2020 (June–August), shows a temperature variation of 13.4 °C to 33.5 °C. The air condition, using evaporative cooling, depicted by the red dots (Fig. 4) shows a maximum of 27.7 °C, indicating that using an evaporator in summer, outdoor air conditions of 27.7 °C or less can be maintained at all times.

4.1.2. p-h graph

A p-h diagram shows the compression of the heat pump cycle with or without evaporative cooling (Fig. 5). The blue line cycle represents the heat pump system without evaporative cooling, and the red dashed cycle represents the heat pump system with evaporative cooling. The condenser setting temperature decreased owing to the evaporation cooling effect of the ambient air after the direct evaporative cooler was operated. The condenser setting temperature is affected by the evaporative cooling. Therefore, the condenser temperature change was determined based on the evaporative cooling effect. The evaporative cooling effect is affected by the wet-bulb temperature of the atmosphere, i.e., the closer the wet-bulb temperature is to the dry-bulb temperature, the less evaporative cooling occurs. The wet-bulb temperature could be replaced by the relative humidity, as the relative humidity approached 100%, the evaporative cooling effect reduced to zero. Therefore, the p-h graph analyze was conducted to examine the change trend in heat pump operation performance due to the evaporative cooling effect during the entire summer. The p-h graph was analyzed when the evaporative cooling effect was the maximum, and the wet-bulb temperature was closest to the dry-bulb temperature, namely the period of highest relative humidity.

Fig. 5(a) shows a p-h diagram in which the highest evaporative cooling effect occurred during summer. The outdoor air condition was 30.35 °C and the relative humidity was 40%. The air cooling temperature after the direct evaporative cooler was 8.404 °C, showing the largest reduction in temperature throughout the summer. To release all heat of refrigerant condensation while satisfying the heat balance, the temperature of the condenser should be set at 70.77 °C. However, it is possible to reduce the temperature of the condenser to a low temperature of 62.33 °C because the cooled air passed through the evaporative cooler into the heat pump. The condenser releases the same heat before the evaporative cooler operates. Fig. 5(b) shows another p-h graph when the highest relative humidity occurred during summer. At this time, the outdoor air condition was 25.35 °C, and the relative humidity was 99%, thus the temperature reduction of the outdoor air was only 0.05 °C. The temperature of the condenser to discharge all the heat of condensation while satisfying the heat balance was 39.64 °C, but even if the evaporative cooler is operated together, the temperature of the condenser modified by the cooled inlet air temperature was 39.59 °C, which is almost the same as before the modification.

Table 4 shows the results for each heat pump parameter, as shown in Fig. 5, and the energy consumption of the heat pump. From the amount of energy savings, it was confirmed that the energy savings were negative for the high humidity conditions shown in Fig. 5(b).

4.2. Energy consumption and COP during summer

The primary energy consumption of the heat-pump system was determined. The heat pump was operated in non-evaporative and full-evaporative cooling modes. The primary energy factor of 2.75 was used for electricity consumption. Non-direct evaporative cooling systems consume 4.05 MWh, with the compressor consuming the maximum energy. In contrast, the fully sprayed heat pump system consumed 3.76 MWh of primary energy during summer. Owing to the improvement in the heat release performance of the condenser, the energy consumed by the compressor of the heat pump was reduced by 290 kWh compared to the non-evaporative cooling mode. The energy consumption of the water pump increased in evaporative cooling mode. This is because the water pump

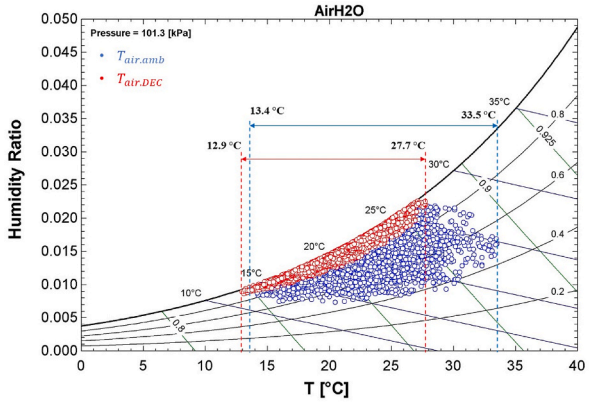

Fig. 4. The hourly air conditions of the ambient air and treated air by the direct evaporative cooler.

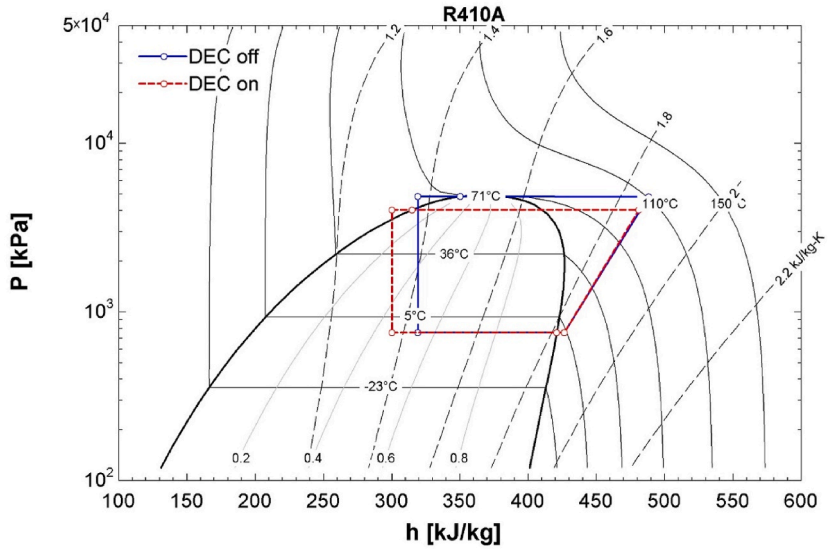

(a) When the highest evaporative cooling performance occurs.

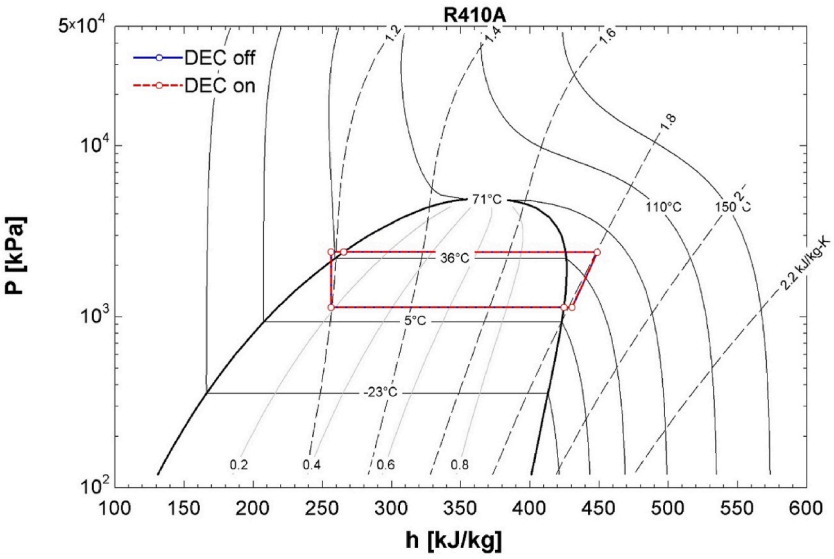

(b) When the highest relative humidity conditions occur.

Fig. 5. p-h graph of the heat pump systems.

Table 4
Parameters of the heat pump shown in the p-h graph.

Figure	T_{oa} [°C]	RH_{oa} [%]	$T_{dec.outlet}$ [°C]	T_{evap} [°C]	T_{cond} [°C]	$T_{cond.new}$ [°C]	ΔT_{oa} [°C]	ΔT_{cond} [°C]	γ_{comp} [−]	$\gamma_{comp.new}$ [−]	$\Delta \dot{W}_{hp.save}$ [kW]
(a)	30.35	40	21	-1.75	70.77	62.33	9.35	8.44	6.42	5.35	1.83
(b)	25.35	99	25.25	11.71	39.64	39.59	0.10	0.05	2.10	2.09	-0.14

is operated to spray water on the top of the evaporative cooling pad.

A box and whisker graph were plotted for the condenser temperature setting, compressor ratio, and the heat pump and system COP to examine the trend of hourly data for the major result parameters of the non-spray and full-sprayed modes (Fig. 6). As shown in Fig. 6

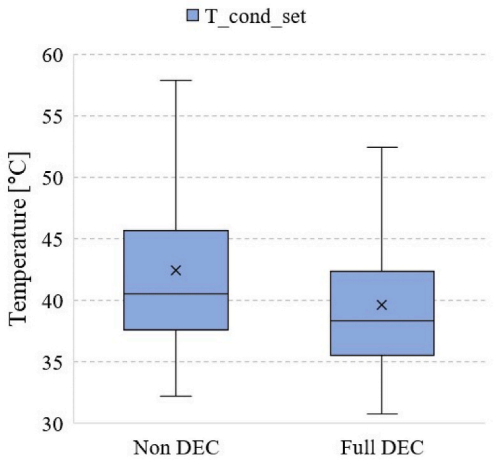

(a) Condenser temperature setting of the heat pump system

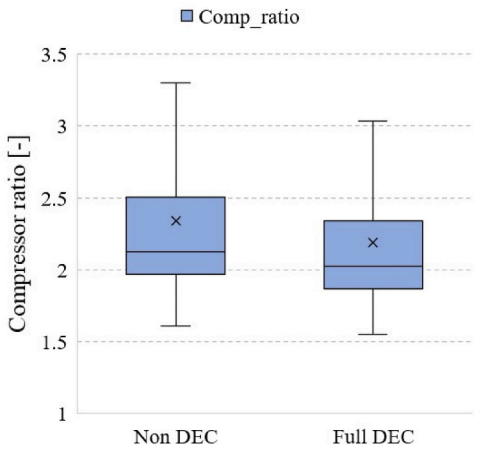

(b) Compressor ratio of the heat pump system

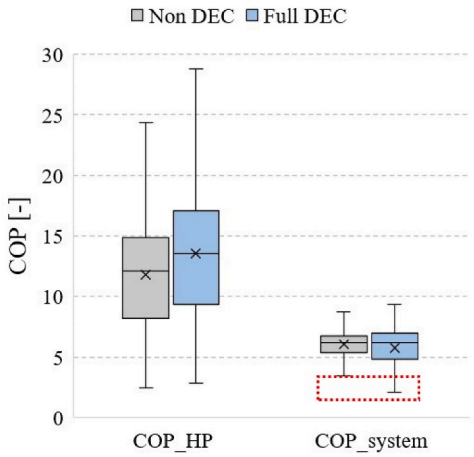

(c) Heat pump and system COP of the heat pump system

Fig. 6. Box plot of parameters for the heat pump system.

(a), for the condenser temperature setting, the range of the non-spray operation was 30.2–57.9 ° C, and the average temperature was 42.4 ° C. The range of the full-spray operation was 30.8–52.46 ° C, and the average temperature was 39.7 ° C. It was confirmed that both the range and the average temperature set for the full-spray-operated heat pump system could be reduced during the summer. This indicates that when operated together with the evaporative cooling system, the heat release performance of the condenser is improved, and thus, a lower temperature can be set.

The reason for the energy-saving effect by modifying the condenser temperature can also be explained by the compression ratio. As shown in Fig. 6(b), the compression ratio of the compressor, for non-spray operation was in the range of 1.6–3.3, and the average compression ratio was 2.3. The range for the full-spray operation was 1.5–3.0, and the average compression ratio was 2.2. It was observed that both the range and average compression ratio of the heat pump during the summer was lower when the full-spray operation was performed. Therefore, the energy is saved during full-spray operation because the reduction in the heat pump compression ratio directly affects the input air.

The reduction in energy consumption compared to the same indoor cooling rate increases the COP of the heat pump and system. As shown in Fig. 6(c), the COP of the heat pump was increased by 14% compared to the non-spray operation, with an average of 11.7 in the case of non-spray, and 13.5 in the case of full-spray. However, energy was lost in the system COP. In the case of non-spray, the range was 3.5–8.7, and the average was 6.0, whereas in the case of full-spray, the range reduced to 2.1–9.3, and the average to 5.7. In addition, the average system COP was reduced by 5%. This energy loss phenomenon shows a tendency similar to the results shown in Table 4. Therefore, it is established that operating the evaporative cooler in a period of high relative humidity has a negative effect on the system energy consumption. Optimal operation requires an effective operation, not just full-spray operation.

4.3. Optimal control point suggestion

4.3.1. Hourly system energy savings

The efficiency of evaporative cooling is reduced under high relative humidity conditions. To determine the energy savings under high relative humidity conditions, a scatter plot of the hourly energy savings for relative humidity is analyzed (Fig. 7). In Fig. 7(a), the x-axis represents the relative humidity, and the y-axis represents the energy savings owing to evaporative cooling. Most of the energy-saving points were positive. However, as the relative humidity approached 100%, negative values were observed (i.e., over-consumption). This indicates that under high relative humidity conditions, energy losses can occur with a slight evaporation cooling effect. As shown in Fig. 7(b), the points of negative values were concentrated at a relative humidity of more than 60%. The lowest over-consumption of energy was 142, which is approximately at the saturation point (i.e., 100% relative humidity).

4.3.2. Optimal energy-saving conditions

Additional energy savings can be achieved by operating the evaporative cooler under low relative humidity conditions, as there is an energy loss when operating at high relative humidity. To find the appropriate evaporative cooling operation point, an iteration flow

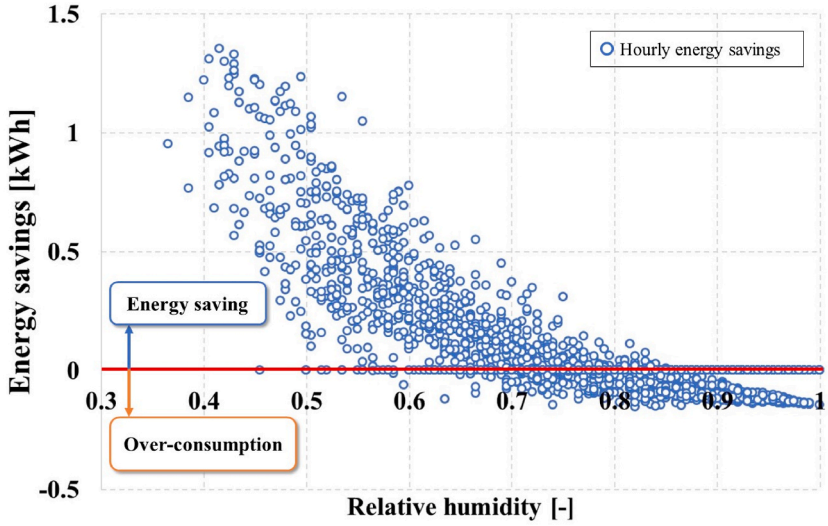

(a). Hourly system energy savings based on relative humidity

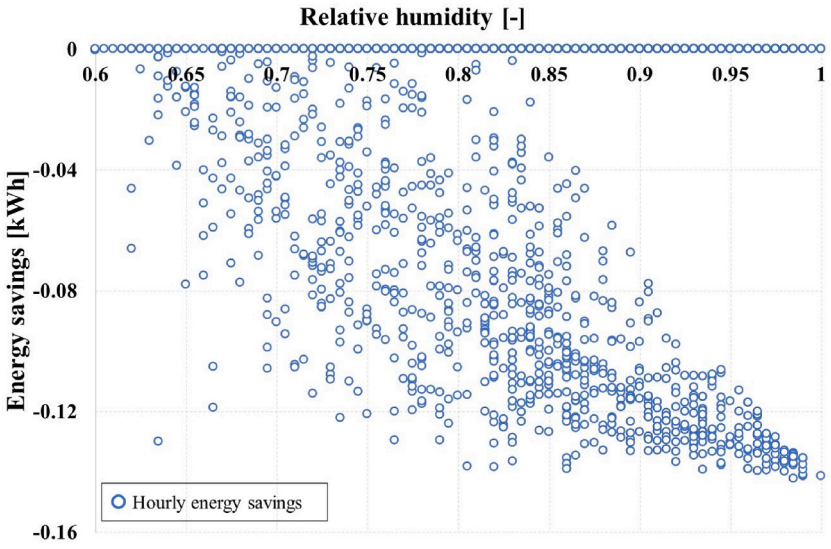

(b). Zoom-in the Figure 7(a) over 0.6 of the relative humidity

Fig. 7. Scatter plot of system energy savings hourly data based on relative humidity.

logic was simulated based on the relative humidity (Fig. 8). First, the energy consumption (P_{sys}) was calculated for the full operation mode (i.e., operation even when the relative humidity is 100% ($x_{rh} = 100\%$)). Subsequently, the energy consumption when the direct evaporative cooler was turned off, was calculated (P_{sys}), based on the assumption that the relative humidity is lowered at each time step ($x_{rh.new}$). The energy consumption was compared with the previous step and the current step. If the consumption at the current step is lower than that of the previous step, iteration is continued until the energy consumption is no longer reduced.

The simulation results showed that 363.8 kWh of energy could be saved when the direct evaporative cooler was operated at 72% relative humidity (Fig. 9). In full-spray operation, energy consumption was 3755.7 kWh lower by 298.4 kWh compared to the non-spray operation, because of on-off control simulation. As the relative humidity decreased, the energy consumption also decreased. The lowest energy consumption of 3690.3 kWh was achieved at 72% relative humidity, thereafter the energy consumption increased. This is the result of the relationship between the evaporative cooling effect and energy consumption of the pump. Under high relative humidity condition, the evaporative cooling effect was negligible, and there was no significant change in the energy consumption of the heat pump. Therefore, the 72% relative humidity condition is an appropriate point between the energy savings and energy consumption of the pump.

4.3.3. Energy consumption and COP in summer

An additional energy simulation was conducted to determine the energy savings achieved by optimal spray operation based on the relative humidity of the outdoor air. Comparing the results of the optimal spray operation mode with the non-spray operation, without evaporative cooler installed and the full-spray operation, the full operation mode saved 7.36%. Whereas the energy savings with, on-off control, at 72% relative humidity was 8.87% (Fig. 10). It was found that 1.63% was further saved when compared to the full-spray

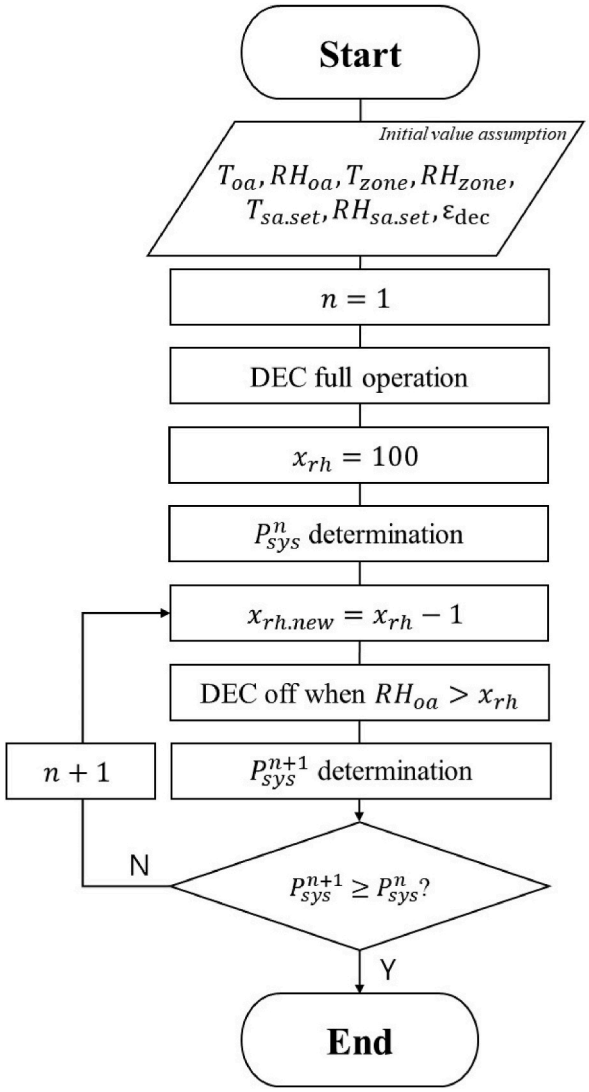

Fig. 8. Flow chart for on-off control of the direct evaporative cooler based on the relative humidity condition.

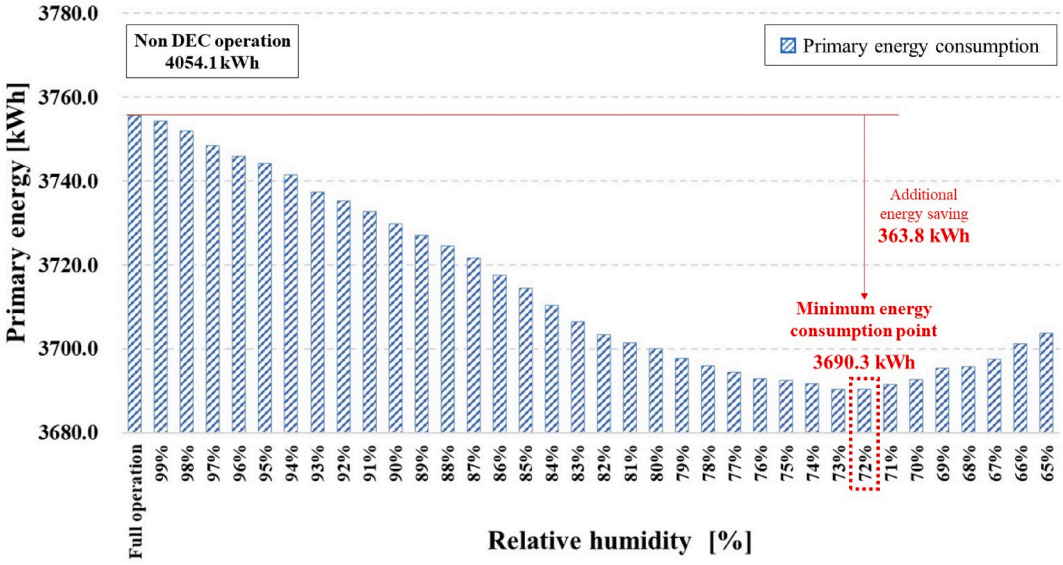

Fig. 9. Primary energy consumption of the proposed system.

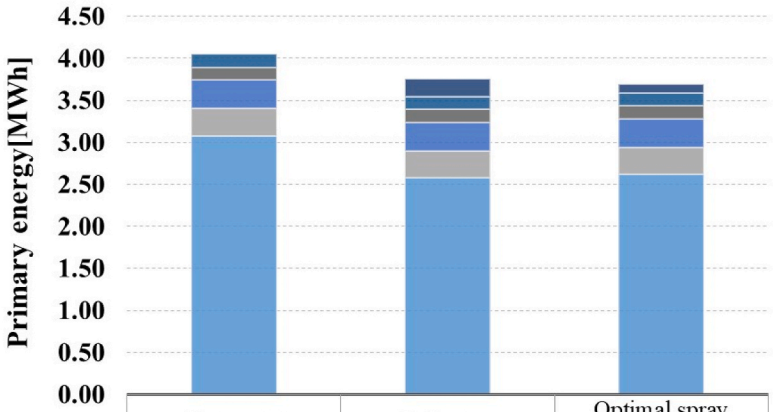

	Non spray	Full spray	Optimal spray (RH<=72%)
P_pump	0.00	0.21	0.10
P_fan_doas_SA	0.16	0.16	0.16
P_fan_doas_RA	0.16	0.16	0.16
P_fan_evap	0.34	0.34	0.34
P_fan_cond	0.32	0.32	0.32
P_compressor	3.08	2.57	2.62

Fig. 10. Primary energy consumption of the heat pump systems.

operation mode.

5. Conclusions

In this study, an energy-saving analysis of an air-source heat pump with a direct evaporative cooling system was evaluated. The results showed that the energy consumption of the system operating with the proposed operation strategy was reduced by 8.87% compared to that of the non-spray operation. Unlike previous studies, when using a heat pump with an evaporative cooling system, the proposed operation logic was utilized considering the time of high-humidity conditions in the outdoor unit. The result shows that the system could reduce the energy consumption with maximum energy efficiency. The heat pump system operated with the proposed operation strategy could save 1.63% more energy than when it is operated in full spray operation without any special operation strategy. The energy-saving effect was the highest when the operation of the evaporative cooler was stopped at a relative humidity of

outdoor air around 72% or higher. Consequently, it is expected that the energy-saving effect will be significant when the evaporative cooler is operated based on a relative humidity of approximately 70–75%. Because the simulation was conducted based on outdoor air conditions in South Korea, it would be necessary to study the systems performance prediction model in various other outdoor conditions.

Author statement

Beom-Jun Kim: Conceptualization, Methodology, Data curation, Writing original draft preparation. **Jae-Weon Jeong**: Supervision, Validation, Reviewing and Editing.

Declaration of competing interest

The authors declare that they have no known competing financial interests or personal relationships that could have appeared to influence the work reported in this paper.

Acknowledgements

This work was supported by the Korea Institute of Energy Technology Evaluation and Planning (KETEP) (No. 20202020800360).

References

[1] W. Grassi, Heat Pumps: Fundamentals and Applications, Springer, 2018.
[2] K.J. Chua, S.K. Chou, W.M. Yang, Advances in heat pump systems: a review, Appl. Energy 87 (2010) 3611–3624, https://doi.org/10.1016/j.apenergy.2010.06.014.
[3] R. Ghoubali, P. Byrne, J. Miriel, F. Bazantay, Simulation study of a heat pump for simultaneous heating and cooling coupled to buildings, Energy Build. 72 (2014) 141–149, https://doi.org/10.1016/j.enbuild.2013.12.047.
[4] L. Ni, J. Dong, Y. Yao, C. Shen, D. Qv, X. Zhang, A review of heat pump systems for heating and cooling of buildings in China in the last decade, Renew. Energy 84 (2015) 30–45, https://doi.org/10.1016/j.renene.2015.06.043.
[5] P. Byrne, J. Miriel, Y. Lénat, Modelling and simulation of a heat pump for simultaneous heating and cooling, Build. Simulat. 5 (2012) 219–232, https://doi.org/10.1007/s12273-012-0089-0.
[6] IPCC, Summary for policymakers, in: V. Masson-Delmotte, P. Zhai, A. Pirani, S.L. Connors, C. Péan, S. Berger, N. Caud, Y. Chen, L. Goldfarb, M.I. Gomis, M. Huang, K. Leitzell, E. Lonnoy, J.B.R. Matthews, T.K. Maycock, T. Waterfield, O. Yelekçi, R. Yu, B. Zhou (Eds.), Climate Change 2021: the Physical Science Basis. Contribution of Working Group I to the Sixth Assessment Report of the Intergovernmental Panel on Climate Change, Cambridge University Press, 2021. In Press.
[7] I.L. Maclaine-Cross, P.J. Banks, A general theory of wet surface heat exchangers and its application to regenerative evaporative cooling, J. Heat Tran. 103 (3) (1983) 579–585, https://doi.org/10.1115/1.3244505.
[8] J.R. Camargo, C.D. Ebinuma, S. Cardoso, A mathematical model for direct evaporative cooling air conditioning system, Rev. Eng. Térmica. 2 (2003) 30, https://doi.org/10.5380/reterm.v2i2.3473.
[9] M. Youbi-Idrissi, H. Macchi-Tejeda, L. Fournaison, J. Guilpart, Numerical model of sprayed air-cooled condenser coupled to refrigerating system, Energy Convers. Manag. 48 (2007) 1943–1951, https://doi.org/10.1016/j.enconman.2007.01.025.
[10] E. Hajidavalloo, H. Eghtedari, Performance improvement of air-cooled refrigeration system by using evaporatively cooled air condenser, Int. J. Refrig. 33 (2010) 982–988, https://doi.org/10.1016/j.ijrefrig.2010.02.001.
[11] K.A. Jahangeer, A.A.O. Tay, M.R. Islam, Numerical investigation of transfer coefficients of an evaporatively-cooled condenser, Appl. Therm. Eng. 31 (2011) 1655–1663, https://doi.org/10.1016/j.applthermaleng.2011.02.007.
[12] P. Sarntichartsak, S. Thepa, Modeling and experimental study on the performance of an inverter air conditioner using R-410A with evaporatively cooled condenser, Appl. Therm. Eng. 51 (2013) 597–610, https://doi.org/10.1016/j.applthermaleng.2012.08.063.
[13] T. Wang, C. Sheng, A.G.A. Nnanna, Experimental investigation of air conditioning system using evaporative cooling condenser, Energy Build. 81 (2014) 435–443, https://doi.org/10.1016/j.enbuild.2014.06.047.
[14] P. Martínez, J. Ruiz, C.G. Cutillas, P.J. Martínez, A.S. Kaiser, M. Lucas, Experimental study on energy performance of a split air-conditioner by using variable thickness evaporative cooling pads coupled to the condenser, Appl. Therm. Eng. 105 (2016) 1041–1050, https://doi.org/10.1016/j.applthermaleng.2016.01.067.
[15] S. Pan, F. Pei, Y. Wei, H. Wang, J. Liu, X. Zhang, G. Li, Y. Gu, Design and experimental study of a novel air conditioning system using evaporative condenser at a subway station in Beijing, China, Sustain. Cities Soc. 43 (2018) 550–562, https://doi.org/10.1016/j.scs.2018.09.013.
[16] H. Yang, L. Rong, X. Liu, L. Liu, M. Fan, N. Pei, Experimental research on spray evaporative cooling system applied to air-cooled chiller condenser, Energy Rep. 6 (2020) 906–913, https://doi.org/10.1016/j.egyr.2020.04.001.
[17] H. Yang, N. Pei, M. Fan, L. Liu, D. Wang, Experimental study on an air-cooled air conditioning unit with spray evaporative cooling system, Int. J. Refrig. 131 (2021) 645–656, https://doi.org/10.1016/j.ijrefrig.2021.06.011.
[18] W. Ketwong, T. Deethayat, T. Kiatsiriroat, Performance enhancement of air conditioner in hot climate by condenser cooling with cool air generated by direct evaporative cooling, Case Stud. Therm. Eng. 26 (2021), 101127, https://doi.org/10.1016/j.csite.2021.101127.
[19] W. Li, W. Shi, J. Wang, Y. Li, J. Lu, Experimental study of a novel household exhaust air heat pump enhanced by indirect evaporative cooling, Energy Build. 236 (2021), 110808, https://doi.org/10.1016/j.enbuild.2021.110808.
[20] B. Shen, J. New, M. Ally, Energy and economics analyses of condenser evaporative precooling for various climates, buildings and refrigerants, Energies 12 (2019), https://doi.org/10.3390/en12112079.
[21] S.Y. Song, H.S. Jin, S.Y. Ha, S.I. Kim, Y.J. Kim, S.J. Lee, I.A. Suh, Detailed office building energy information based on in situ measurements, Energies 13 (2020), https://doi.org/10.3390/en13123050.
[22] M.H. Kim, J.W. Jeong, Cooling performance of a 100% outdoor air system integrated with indirect and direct evaporative coolers, Energy 52 (2013) 245–257, https://doi.org/10.1016/j.energy.2013.02.008.
[23] J.W. Jeong, S.A. Mumma, W.P. Bahnfleth, Energy conservation benefits of a dedicated outdoor air system with parallel sensible cooling by ceiling radiant panels, ASHRAE Trans. 109 PART 2 (2003) 627–636.
[24] ASHRAE, ANSI/ASHRAE, Standard 55-2020, Thermal Environmental Conditions for Human Occupancy, Inc., 2020.
[25] J.W. Mitchell, J.E. Braun, Principles of Heating, Ventilation, and Air Conditioning in Buildings, John Wiley & Sons, 2012.
[26] M.H. Kim, J.H. Kim, O.H. Kwon, A.S. Choi, J.W. Jeong, Energy conservation potential of an indirect and direct evaporative cooling assisted 100% outdoor air system, Build. Serv. Eng. Technol. 32 (2011) 345–360, https://doi.org/10.1177/0143624411402637.
[27] ASHRAE, ANSI/ASHRAE, Standard 62.1-2019, Ventilation for Acceptable Indoor Air Quality, Inc., 2019.
[28] ASHRAE, ANSI/ASHRAE, Standard 90.1-2019, Energy Standard for Buildings except Low-Rise Residential Buildings, Inc., 2019.

[29] Korea Energy Agency, Ministry of Land, Infrastructure and Transport, Republic of South Korea, Energy saving design standard of buildings, 2018.
[30] S.A. Klein, et al., TRNSYS 18: A Transient System Simulation Program, Solar Energy Laboratory, University of Wisconsin, Madison, USA, 2017. http://sel.me.wisc.edu/trnsys.
[31] Munters Evaporative, Cooling with CELdek, Technical Manual, CELdek® 7060-15 Available online: http://www.munters.com. (Accessed 15 December 2021).
[32] B. Givoni, Passive and Low Energy Cooling of Buildings, John Wiley & Sons, 1994.
[33] G. Chiesa, M. Grosso, Direct evaporative passive cooling of building. A comparison amid simplified simulation models based on experimental data, Build. Environ. 94 (2015) 263–272, https://doi.org/10.1016/j.buildenv.2015.08.014.
[34] U.S. Department, Of Energy. Building Technologies Program, U.S. Department of Energy, Washington, DC, USA, 2021.
[35] N.M. Phu, N. Van Hap, Influence of inlet water temperature on heat transfer and pressure drop of dehumidifying air coil using analytical and experimental methods, Case Stud. Therm. Eng. 18 (2020), 100581, https://doi.org/10.1016/j.csite.2019.100581.
[36] J. Woods, E. Kozubal, Heat transfer and pressure drop in spacer-filled channels for membrane energy recovery ventilators, Appl. Therm. Eng. 50 (2013) 868–876, https://doi.org/10.1016/j.applthermaleng.2012.06.052.
[37] EnergyPlus Engineering Reference, Version 22.1.0, DOE, 2022. Available online: https://energyplus.net/. (Accessed 9 April 2022).